

Calibration of the two microphone transfer function method to measure acoustic impedance in a wide frequency range

R. Boonen¹, P. Sas¹, W. Desmet¹, W. Lauriks², G. Vermeir²

¹ K.U.Leuven, Department of Mechanical Engineering,
Celestijnenlaan 300 B, B-3001, Heverlee, Belgium

² K.U.Leuven, Department of Acoustics and Thermal Physics,
Celestijnenlaan 200 D, B-3001, Heverlee, Belgium

e-mail: rene.boonen@mech.kuleuven.be

Abstract

In many acoustic simulations, particularly when using lumped parameter models or electrical analog circuits, the acoustic impedance of a component needs to be determined accurately. A widely used acoustic impedance measurement method is the "two microphone transfer function method", which is standardized in ISO-10534-2. When the acoustic impedance is needed over a wide frequency band, for example from 10Hz to 10kHz, this method faces some limitations. In this paper, a new calibration method will be proposed such that acoustic impedances can be measured with high accuracy over a wide frequency range. The estimation of the speed of sound has been eliminated. Using the measured transfer functions between the two sensors at two different reference sections, the sensor positions will be accurately calibrated. The calibration of the sensor mismatch has become superfluous, so interchanging positions of the sensors is not necessary. A recursive procedure has been proposed to maximize the microphone position accuracy. The resulting calibration procedure has been reduced to the accurate determination of the sensor positions.

1 Introduction

A proper design of acoustic systems involving components such as silencers, resonators, absorbing materials, horns, etc . . . , requires an accurate acoustic characterization of the various components. Such systems can be simulated using lumped element models or electrical analog circuits. The accuracy of the simulation result depends on the accuracy of the acoustic impedance of each component. Therefore, accurate acoustic impedance measurement methods are mandatory.

The most straight forward technique uses a pressure and a volume velocity sensor [1], whereby the impedance is calculated directly from the ratio between both measured quantities. The direct measurement of the volume velocity can be carried out using for example a hot wire anemometer. Another approach is using an excitation source with a known volume velocity.

Other methods are based on connecting known impedances to the impedance to be measured. These methods are mostly used to determine the internal acoustic impedance of a source [2, 3, 4]. To the impedance to be measured, known acoustic loads are connected and the response to the source is measured. A set of equations results, from which the unknown impedance can be quantified. However, the equation set is often ill-conditioned and provides inaccurate impedance results.

A common acoustic impedance measurement technique is the standing wave ratio (SWR) method (the classical Kundt duct). This method is described in the ISO-10534-1 standard. The ends of the Kundt duct are closed by an excitation source at one end and the unknown impedance at the other end. The source generates a sinusoidal signal which results in a standing wave pattern in the duct. A microphone is moved along the axis

of the duct. The minimum and maximum pressure amplitude of the standing wave and the location where the minimum and maximum amplitude occur are determined. From these data, the reflection coefficient and the acoustic impedance are calculated.

Another common method is the "two microphone transfer function method", which is described in ISO-10534-2. This method uses the transfer function measured between two pressure sensors at two distinct positions in the measurement wave guide to determine the acoustic impedance attached at one side of the wave guide. This method is discussed in more detail in the next section.

When the acoustic impedance is needed over a wide frequency band, for example from 10Hz to 10kHz, all the previously described impedance measurement methods face some limitations. Therefore, a new calibration method is under investigation which allows acoustic impedances to be measured with high accuracy over a wide frequency range. The new method does not require the measurement of the speed of sound. The interchanging of the pressure sensors has been avoided using two calibration impedances. Consequently, the calibration of the sensor mismatch is not required. A recursive procedure is proposed to refine the microphone position calibration. This refinement can be repeated until the maximum calibration accuracy is reached. The new method includes wave guide damping to enhance accuracy.

2 The two microphone transfer function method.

This section discusses the principle of the two microphone transfer function method including wave guide damping. Figure 1 presents the setup for acoustic impedance measurement. The setup consists of a straight duct which is the measurement acoustic wave guide. At the left end, an excitation source, such as a loudspeaker, is connected. At the right end, the impedance to be measured is connected. This impedance includes everything present at the right side of the reference section. Two microphones at two distinct positions x_1 and x_2 measure the sound pressure inside the duct. From the transfer function between the two microphones, the reflection coefficient and consequently, the unknown connected impedance will be determined.

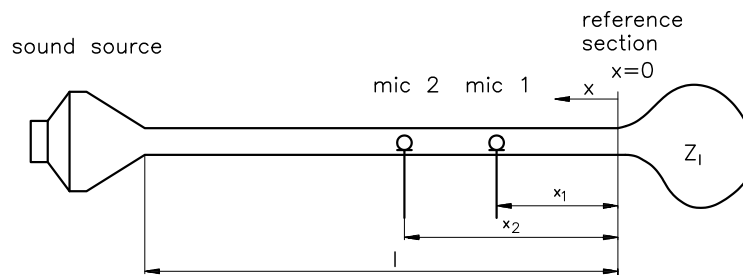


Figure 1: Wave guide with an unknown acoustic impedance Z_1 .

Wave attenuation is caused by three different mechanisms. These are wall friction, heat exchange and internal gas viscosity [8]. The wave guide dimensions determine the dominant attenuation mechanism. In the frequency domain, the wave guide damping can be approximated by introducing a constant loss factor ξ in the compressibility κ of the medium [9]:

$$\kappa \approx \kappa_0 (1 + j2\xi) \quad (1)$$

wherein $j = \sqrt{-1}$ and κ_0 is the lossless compressibility of the medium. This type of loss factor is frequency independent and will not cause dispersion. This damping mechanism provides a good fit with the measured transfer functions in a wide frequency range.

The effect of the loss factor ξ on the characteristic impedance Z_0 of the wave guide and the propagation

constant γ is:

$$Z_0 \approx \sqrt{\frac{\rho_0 \kappa_0}{S^2}} (1 + j\xi) \quad \text{and} \quad \gamma \approx \omega \sqrt{\frac{\rho_0}{\kappa_0}} (1 + j\xi) \quad (2)$$

wherein ρ_0 is the density of the medium and S is the cross-section of the wave guide.

The wave pattern in the wave guide is governed by the one-dimensional Helmholtz wave equation, which describes the pressure distribution along the wave guide. At each position x , the pressure in terms of the propagation constant γ in the wave guide equals [7]:

$$p(x, \gamma) = \phi_g \frac{Z_0 Z_g}{Z_0 + Z_g} \cdot \frac{e^{-j\gamma l}}{1 - \Gamma_l \Gamma_g e^{-j2\gamma l}} \cdot (e^{j\gamma x} + \Gamma_l e^{-j\gamma x}) \quad (3)$$

wherein ϕ_g is the source volume velocity, Z_g the source internal impedance, l the distance between the exciting sound source and the reference section, Γ_l and Γ_g the reflection coefficients at the load side and source side respectively.

To measure the load impedance using the two microphone method, the transfer function T_{12} between the pressures at two distinct positions x_1 and x_2 is taken:

$$T_{12} = \frac{p(x_1, \gamma)}{p(x_2, \gamma)} = \frac{e^{j\gamma x_1} + \Gamma_l e^{-j\gamma x_1}}{e^{j\gamma x_2} + \Gamma_l e^{-j\gamma x_2}} \quad (4)$$

Notice that the source reflection coefficient drops out, the reflection coefficient at the load is the single unknown. Consequently, the choice of the source type is free. The load reflection coefficient Γ_l will then be isolated from equation (4) and the load impedance Z_l results from:

$$Z_l = Z_0 \frac{1 + \Gamma_l}{1 - \Gamma_l} = jZ_0 \frac{\sin \gamma x_1 - T_{12} \sin \gamma x_2}{\cos \gamma x_1 - T_{12} \cos \gamma x_2} \quad (5)$$

3 Calibration of the set-up according to ISO 10534-2

Equation (5) becomes inaccurate when the reflection coefficient Γ_l approaches unity. This situation occurs when the unknown impedance deviates largely from the characteristic impedance of the wave guide. Therefore, prior calibration of the setup is necessary to obtain accurate results.

The ISO 10534-2 standard demands the following calibration actions:

- The velocity of sound needs to be determined accurately using measurements of ambient temperature and atmospheric pressure.
- The distance between the pressure sensors needs to be measured accurately.
- The mismatch between the amplitude and phase of the pressure sensors needs to be calibrated. In short, the procedure is to measure the transfer function T_{12} of the two pressures at position x_1 and x_2 , then interchange the two pressure sensors from location x_1 to x_2 and from x_2 to x_1 respectively, measure the transfer function T_{21} and calculate the calibration factor δ such that:

$$\delta^2 T_{12} T_{21} = 1 + 0j \quad (6)$$

This calibration factor δ is complex and frequency dependent.

In order to illustrate the accuracy of the ISO calibration procedure, a simulation with representative data for such setup is carried out [10].

Suppose the wave guide has a diameter of 40 mm, the characteristic impedance will be $Z_0 = 320 \text{ k}\Omega$ ($1 \text{ }\Omega = 1 \text{ Pa s/m}^3$). The distance between the nearest pressure sensor and the reference section is $x_1 = 0.2 \text{ m}$ and between the farthest pressure sensor and the reference section $x_2 = 0.5 \text{ m}$. Suppose the impedance measurement range is limited to 120 dB (ref. Z_0), i.e. 60 dB above and below Z_0 , the closed duct ("infinite") impedance Z_l will be limited to $1000Z_0$. When determining the reversed transfer function T_{21} after interchanging the sensors, position deviations of 0.5 mm have been introduced on the distances x_1 and x_2 . These deviations are realistic, due to tolerances on the mounting hole and the position of the acoustic centre of the sensor.

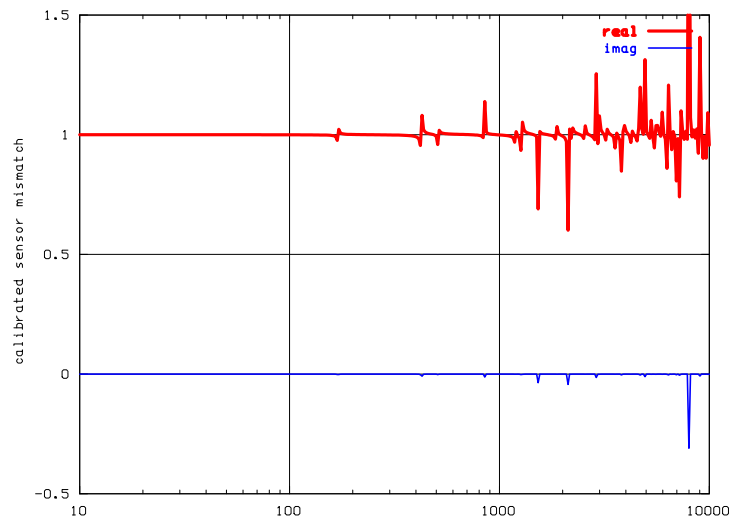


Figure 2: Calibration result of the pressure sensors according to ISO 10534-2.

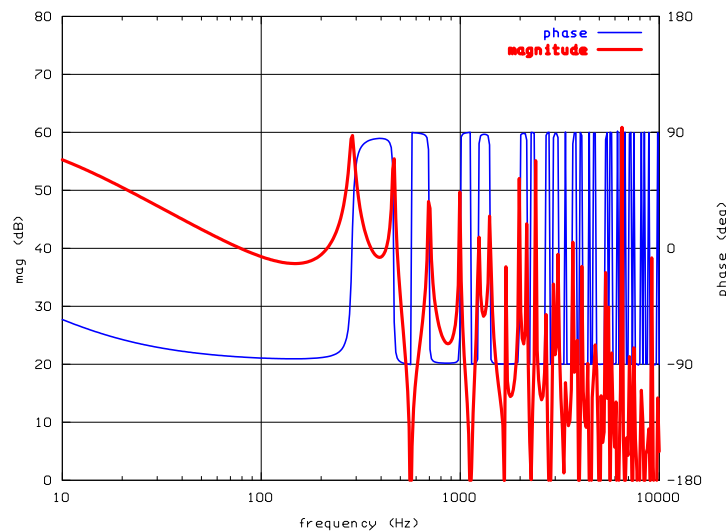


Figure 3: Resulting closed duct end impedance using the calibration data displayed in figure 2(left).

The calibration method described in the ISO 10534-2 standard is applied. The resulting calibration factor δ times the sensor mismatch is presented in figure 2. This product should equal $1 + 0j$. In the lower frequency range, the calibration has been successful. However, in the higher frequency range, starting from 150 Hz, the calibration is erroneous and even worse than the uncalibrated situation. The resulting closed duct impedance is presented in figure 3. This should be a straight line at 60 dB, but due to the erroneous calibration, large deviations results. In this case, the measurement range wherein the unknown impedance can be reliably measured is limited to 35 dB around Z_0 until 400 Hz. Above 400 Hz, reliable impedance measurements are

not possible. This simulation demonstrates that it will be necessary to calibrate the pressure sensor positions accurately.

4 Improved calibration method

This paper proposes an improved calibration procedure. The new method focusses on the accurate determination of the sensor positions, expressed as the travelling times of the acoustic waves from the respective sensor positions to the reference section. The effect of the wave damping is substantial and is taken into account.

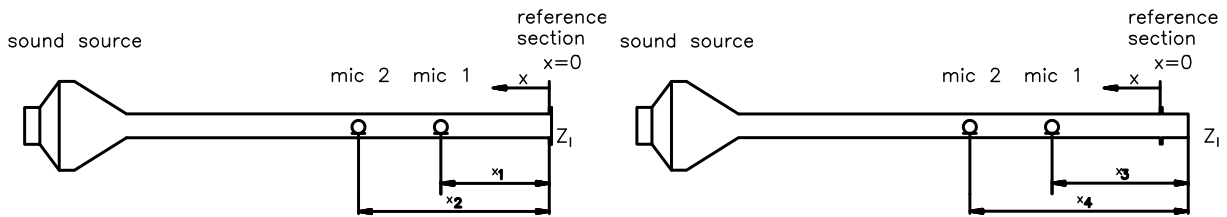


Figure 4: Left: calibration setup with duct end closed at the reference section and right: closed at the shifted reference section.

The laboratory setup, presented in figure 5, consists of a duct of 40 mm internal diameter and 2 m length equipped with a 60 W horn driver. The sensors are positioned at a distance $x_1 = 0.3$ m and $x_2 = 0.47$ m from the reference section. Two transfer functions are measured between the two sensor outputs. The first transfer function T_{12} is measured with the duct closed at the reference section, as presented in figure 4(left). An additional piece of duct of 46 mm length is added resulting in a shift of the reference section, as presented in figure 4(right). The second transfer function T_{34} is measured. The resulting transfer functions T_{12} and T_{34} are represented in figure 6 and figure 7 respectively. All calibration information will be extracted from these transfer functions. Finally, a recursive refinement procedure will maximize the accuracy of the position calibration.



Figure 5: Laboratory setup for acoustic impedance measurement.

4.1 Elimination of the speed of sound.

The distances x_1, x_2, x_3 and x_4 can be substituted by the travelling times t_1, t_2, t_3 and t_4 needed for the wave to travel from these positions to their reference sections respectively. The relation between the travelling times

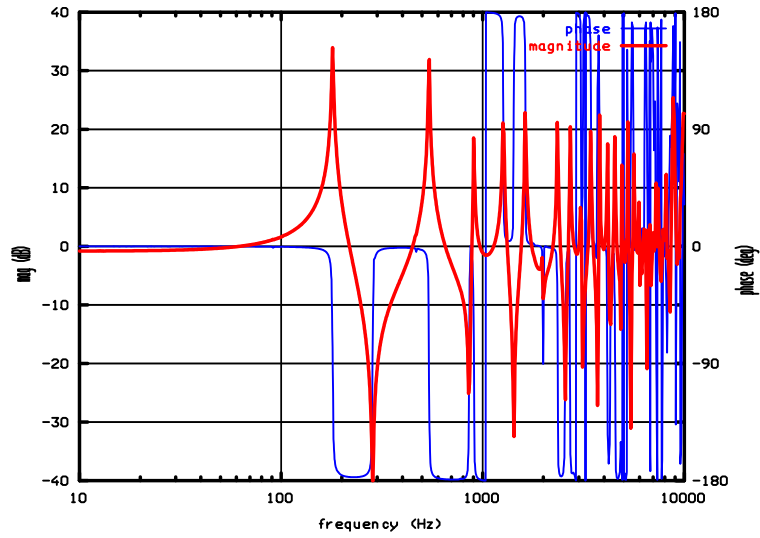


Figure 6: Measured transfer function T_{12} between the sensors with the duct closed at the reference section.

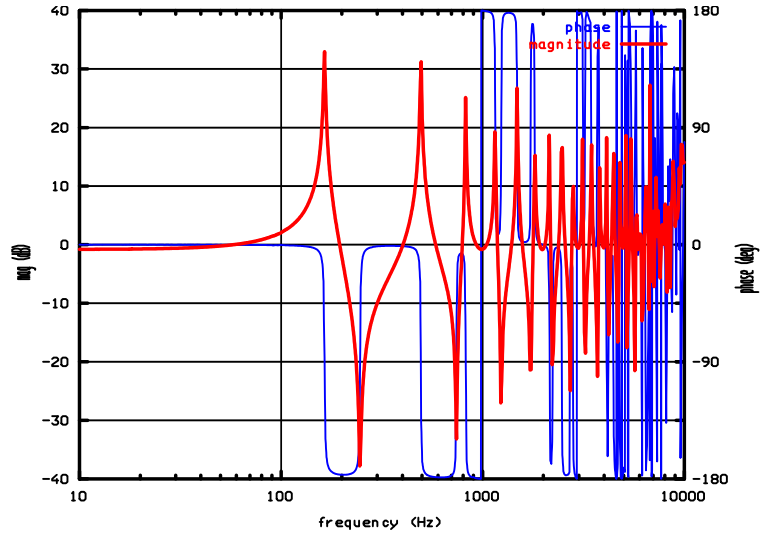


Figure 7: Measured transfer function T_{34} between the sensors with the duct closed at the shifted reference section.

and their respective distances is:

$$t_i = \frac{x_i}{v_{\text{ph}}} \quad (i = 1, 2, 3, 4) \quad (7)$$

wherein $v_{\text{ph}} = \frac{\omega}{\text{Re}(\gamma)}$ is the phase velocity of the sound. It is a real value. The resulting transfer functions T_{12} and T_{34} in terms of travelling times will be:

$$\begin{aligned} T_{12} &= \frac{\delta (Z_c \cos \beta t_1 + j Z_0 \sin \beta t_1)}{(Z_c \cos \beta t_2 + j Z_0 \sin \beta t_2)} \\ T_{34} &= \frac{\delta (Z_c \cos \beta t_3 + j Z_0 \sin \beta t_3)}{(Z_c \cos \beta t_4 + j Z_0 \sin \beta t_4)} \end{aligned} \quad (8)$$

wherein $\beta = \omega (1 + j \xi)$.

The travelling times t_1 and t_2 are estimated from the measured transfer function T_{12} (figure 6), t_3 and t_4 from the transfer function T_{34} (figure 7). They correspond to the first pole for the farthest microphone and the first zero for the nearest microphone position. The pole and the zero correspond to the first node of the pressure distribution of the standing wave appearing at the positions x_1, x_2, x_3 and x_4 respectively. These travelling times t_1, t_2, t_3 and t_4 equal:

$$t_1 = \frac{1}{4f_1} \quad , \quad t_2 = \frac{1}{4f_2} \quad , \quad t_3 = \frac{1}{4f_3} \quad \text{and} \quad t_4 = \frac{1}{4f_4} \quad (9)$$

in which the frequencies f_1, f_2, f_3 and f_4 are associated to the frequencies determined by the quarter wavelength between the reference section and the positions x_1, x_2, x_3 and x_4 respectively.

4.2 Elimination of the sensor mismatch.

By considering the ratio between the two measured transfer functions T_{12} and T_{34} , the sensor mismatch vanishes from numerator and denominator:

$$\begin{aligned} T_c &= \frac{T_{12}}{T_{34}} = \frac{\delta(Z_c \cos \beta t_1 + jZ_0 \sin \beta t_1)}{(Z_c \cos \beta t_2 + jZ_0 \sin \beta t_2)} \cdot \frac{(Z_c \cos \beta t_4 + jZ_0 \sin \beta t_4)}{\delta(Z_c \cos \beta t_3 + jZ_0 \sin \beta t_3)} \\ &= \frac{Z_c^2 \cos \beta t_1 \cos \beta t_4 - Z_0^2 \sin \beta t_1 \sin \beta t_4 + jZ_c Z_0 \sin \beta t_1 \cos \beta t_4 + jZ_c Z_0 \cos \beta t_1 \sin \beta t_4}{Z_c^2 \cos \beta t_2 \cos \beta t_3 - Z_0^2 \sin \beta t_2 \sin \beta t_3 + jZ_c Z_0 \sin \beta t_2 \cos \beta t_3 + jZ_c Z_0 \cos \beta t_2 \sin \beta t_3} \end{aligned} \quad (10)$$

Figure 8 presents the ratio T_c between the measured transfer functions T_{12} and T_{34} .

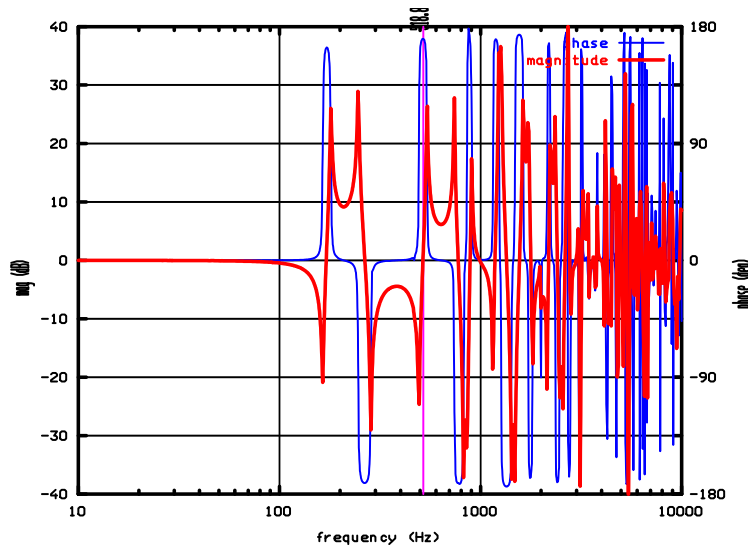


Figure 8: Division of the two transfer functions $T_c = T_{12}/T_{34}$

4.3 Determining the wave guide damping.

If the wave guide is ideally closed, the transfer function given in equation (10) simplifies to:

$$T_{c0} = \frac{\cos \beta t_1 \cos \beta t_4}{\cos \beta t_2 \cos \beta t_3} \quad (11)$$

The ratio between the transfer function T_{c0} and the measured transfer function T_c is very small and is presented in figure 9. At certain frequencies, the transfer functions T_{c0} and T_c are equal. There, the loss factor ξ

is the only unknown and will be determined numerically from $T_c - T_{c0} = 0$. When the phase has an extremum at this frequency, the loss factor can be most accurately determined. In figure 9, the first frequency where both conditions are fulfilled is 518.8 Hz. Consequently, the loss factor is evaluated at that frequency.

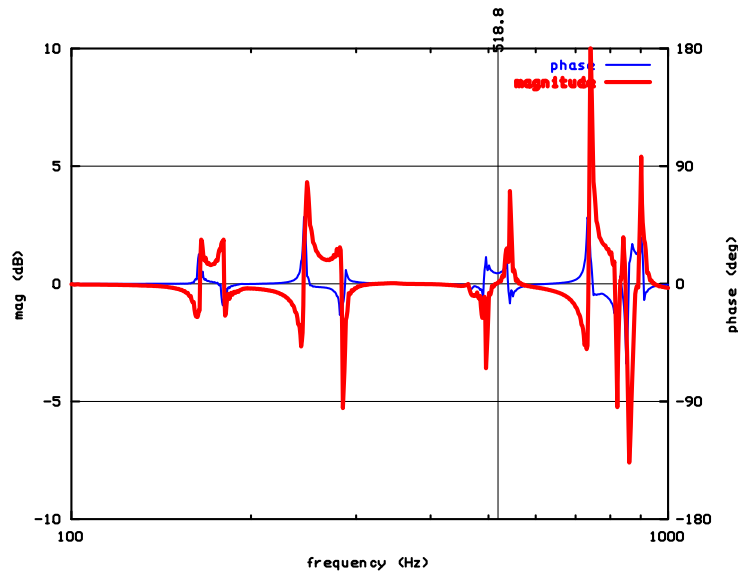


Figure 9: Ratio between the measured transfer function T_c and the ideally closed wave guide transfer function T_{c0} .

4.4 Determining the closed end impedance.

After introducing the loss factor ξ in the transfer function T_c expressed by equation (10), the acoustic impedance Z_c of the closed end can be determined from the measured transfer function presented in figure 8. The resulting impedance, presented in figure 10, is the closed end impedance and defines the measurement range. It must be as large as possible. The expression (10) is quadratic in Z_c , resulting in two solutions. One solution corresponds to the direct reference section, the other to the shifted reference section. It is necessary to select the proper solution at each frequency point.

4.5 Refining the sensor positions.

Often, the travelling times t_1 , t_2 , t_3 and t_4 are still not sufficiently accurate when determined from the equations (9). The impedance is extremely sensitive to errors in the travelling times. Therefore, the acoustic impedance Z_c of the closed duct itself will be used to refine these travelling times.

The impedance measurement is only correct if the distance between the two microphones is correct. An exception occurs at distinct frequencies, when a half wave length stands between one of the sensors and the closed reference section, as presented in figure 11. A pressure maximum occurs at one of the microphone positions, the gradient of the pressure is zero and a small deviation of the microphone position does not affect the accuracy of the measured impedance. The impedance occurring at these frequencies, consist of a short wave guide with closed end with length Δx_1 if the pressure maximum is situated at x_2 or with length Δx_2 if the pressure maximum is situated at x_1 .

Expressed in travelling time, the correction of t_1 will be executed at the frequency $f_2 = \frac{1}{2t_2}$ and the correction of t_2 at $f_1 = \frac{1}{2t_1}$. The travelling time corrections τ_1 and τ_2 are the times needed for the sound wave to travel

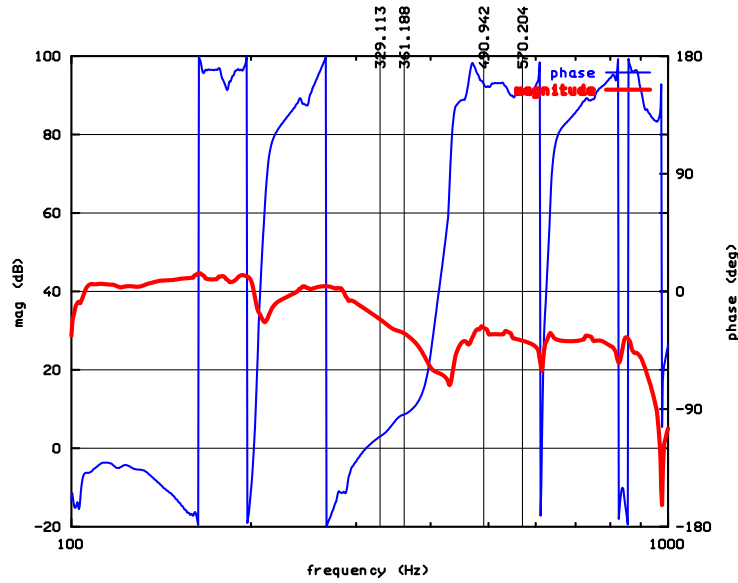


Figure 10: Resulting closed end impedance Z_c (dB(ref Z_0)) applying expression (10) to the measured transfer function T_c .

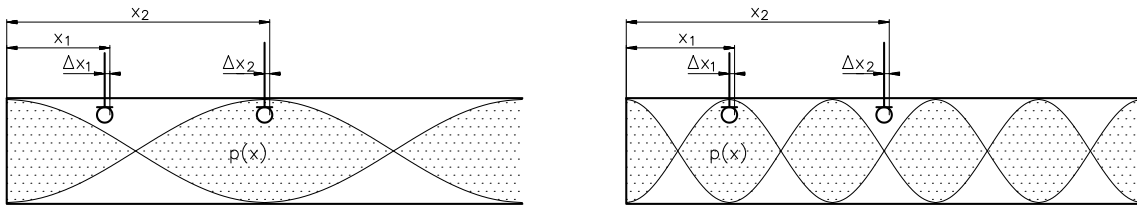


Figure 11: Refining situations for x_1 and x_2 .

the distances Δx_1 and Δx_2 respectively:

$$\tau_i = \frac{t_2}{\pi} \arctan \frac{Z_0}{jZ_{c2}} \quad \text{and} \quad \tau_2 = \frac{t_1}{\pi} \arctan \frac{Z_0}{jZ_{c1}} \quad (12)$$

in which Z_{c2} is the measured closed end impedance Z_c evaluated at f_2 and Z_{c1} evaluated at f_1 . In the same way, the travelling times t_3 and t_4 are corrected. The closed end impedance Z_c can be recalculated using these corrected travelling times. The correction of the travelling times can be repeated until the maximum accuracy has been reached. Figure 12 demonstrates how the closed end impedance increases about 10 dB, compared to figure 10, resulting in a higher impedance magnitude measurement range. The frequencies whereby the position refinement has been carried out are $f_1 = 567$ Hz, $f_2 = 361$ Hz, $f_3 = 489$ Hz and $f_4 = 329$ Hz, which are displayed in figure 10 and figure 12.

5 Determining unknown impedance

After calibration, the unknown impedance needs to be determined. For that purpose, the unknown impedance is connected on the wave guide at the reference section and the transfer function T_l between the microphones is measured. The following data resulting from the calibration procedure are needed: T_{34} , Z_c , t_1 , t_2 , t_3 , t_4 and ξ . The unknown impedance Z_l is then obtained from:

$$Z_l = Z_0 \frac{Z_0 (\sin \beta t_1 \sin \beta t_4 - T \sin \beta t_2 \sin \beta t_3) + jZ_c (T \sin \beta t_2 \cos \beta t_3 - \sin \beta t_1 \cos \beta t_4)}{Z_c (T \cos \beta t_2 \cos \beta t_3 - \cos \beta t_1 \cos \beta t_4) + jZ_0 (\cos \beta t_1 \sin \beta t_4 - T \cos \beta t_2 \sin \beta t_3)} \quad (13)$$

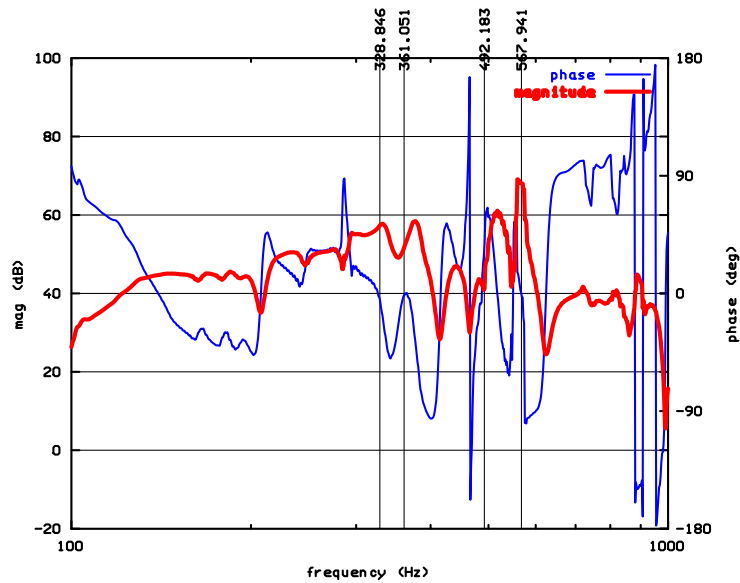


Figure 12: Resulting closed end impedance after refining travelling times.

wherein $T = T_1/T_{34}$.

As an example, figure 13 presents the open end impedance, calibrated using the new method. The smooth lines represent the analytical spherical radiator impedance [6].

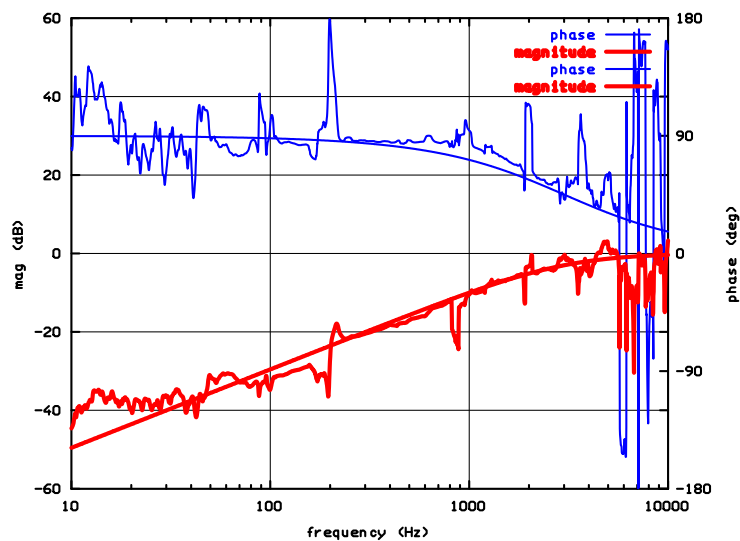


Figure 13: Resulting open end impedance after improved calibration.

To further improve the measurement method, other error sources will be investigated, such as finite sensor dimensions and transfer function amplitude variations.

6 Conclusion

A new calibration method is proposed to measure acoustic impedances with high accuracy over a wide frequency range. The estimation of the speed of sound is no longer required. Consequently, the temperature and ambient pressure measurements are not necessary. Using the measured transfer functions between the

two sensors for two different reference sections, the sensor positions can be accurately calibrated. These sensor positions are further refined using a recursive procedure. The calibration of the sensor mismatch has become superfluous, so exchanging positions of the sensors is no longer needed. The accuracy of the impedance measurement method has been enhanced by including the wave guide damping in the calibration procedure.

References

- [1] J.-P. Dalmont, *Acoustic impedance measurement, part I, A review*. Journal of Sound and Vibration, Vol. 243, No. 3, (2001), pp. 441-459.
- [2] M. G. Prasad, *A four load method for evaluation of acoustic source on a duct*, Journal of Sound and Vibration, Vol. 114, No. 2, (1987), pp. 347-356.
- [3] L. Desmons, J. Hardy and Y. Auregan, *Determination of the acoustic source characteristics of an internal combustion engine by using several calibrated loads*. Journal of Sound and Vibration, Vol. 179, No. 5, (1995), pp. 869-878.
- [4] H. Bodén, *On multi-load methods for determination of the source data of acoustic one-port sources*. Journal of Sound and Vibration, Vol. 180, No. 5, (1995), pp. 725-743.
- [5] ISO 10534-2, *Determination of sound absorption coefficient and impedance in impedance tubes*, International Organisation for Standardization, Case postale 56, CH-1211 Genève 20, (1998).
- [6] L. L. Beranek, *Acoustics*, Mc Graw-Hill, (1954)
- [7] H. P. Neff, Jr, *Basic Electromagnetic Fields*, Harper & Row, (1987)
- [8] A. D. Pierce, *Acoustics: An introduction to its physical principles and applications*, Mc-Graw-Hill, (1981)
- [9] E.J. Scudrzyk, *Foundations of Acoustics*, Springer Verlag (1972)
- [10] R. Boonen, P. Sas, *Calibration of the two microphone transfer function method to measure acoustic impedance in a wide frequency range*. Proceedings of The ISMA2004 Conference, Leuven, Belgium, Vol I, (2004), pp. 325-336.
- [11] R. Boonen, P. Sas, *Determination of the acoustic impedance of an internal combustion engine exhaust*. Proceedings of The ISMA2002 Conference, Leuven, Belgium, Vol V, (2002), pp. 1939-1946.

